ARTICLE

Free-Standing Phytantriol Q^{224} Cubic Phase Films: Resistivity Monitoring and Switching

Rosemary Brown,[a,b] Elena Madrid,[b] Remi Castaing,[b] James M. Stone,[a] Adam M. Squires,[c] Karen J. Edler,[b] Kei Takashina,[a] Frank Marken [b]*

Abstract: Phytantriol Q^{224} cubic phase, as a bi-continuous meso-structured material stable in contact with aqueous electrolyte, has found applications in drug delivery and cosmetics and is employed here as a free-standing film separating two aqueous compartments in order to study (i) ion conductivity (at low potential bias within ±0.8 V), (ii) conductivity switching effects (at high potential bias beyond ±0.8 V), and (iii) phase switching effects (as a function of temperature). A microhole of approximately 20 μm diameter in a 6 μm thick poly-ethylene-terephthalate (PET) film is employed as support coated with phytantriol (on a single side or on both sides) in contact with aqueous electrolyte phase on both sides in a classic 4-electrode measurement cell. The conductivity of the phytantriol phase within the microhole is shown to be ionic strength, applied potential, time/history, and temperature dependent. The experimental data for asymmetric phytantriol deposits are indicative of a microhole resistance that can be switched between two states (high and low resistance associated with a filled or empty microhole, respectively). When heating symmetrically applied films of phytantriol, Q^{224} to H_{II} phase transition linked to a jump to higher specific resistivity is observed consistent with differential scanning calorimetry (DSC) data for this phase transition.

Introduction

Polar lipids in water form a variety of self-assembled structures[1] with applications such as templates for example for metals,[2] polymers,[3] in protein encapsulation,[4] or in drug delivery.[5,6] One of these structures, the bi-continuous cubic phase, is of particular interest as it consists of two non-intersecting continuous water channels (see Figure 1A).[7] The water channels twist in three dimensions and are separated by a lipid layer creating a liquid crystalline structure. Applications of this type of self-assembled structure have been suggested in drug-delivery or in biosensing[8] and work has been reported by Mezzenga and coworkers on quantitative understanding of diffusion processes in free-standing lyotropic phases,[9] light-triggered drug release,[10] pH-responsive lyotropic liquid crystals,[11,12] magnetic field switchable mesophase channels,[13] and water channel tuning with sucrose stearate.[14,15]

Phytantriol (or 3,7,11,15-tetramethyl-1,2,3-hexadecanetriol, see structure in Figure 1B inset) forms stable cubic mesophases in the presence of excess water.[16] It assumes the well-known gyroid and double diamond cubic mesophases with space groups Ia3d and $Pn\bar{3}m$ (= Q^{224}), respectively. The experimental SAXS pattern for the $Pn\bar{3}m$ structure of the Q^{224} phytantriol phase is shown in Figure 1B. Figure 1A shows the corresponding water and lipid channel structure of the mesophase.

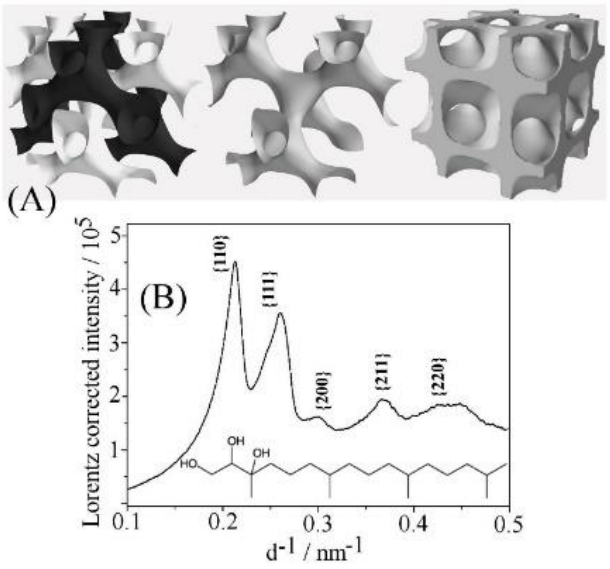

Figure 1. (A) The $Pn\bar{3}m$ structure of the Q^{224} bi-continuous cubic mesophase of phytantriol showing the two independent water channel systems, a single water channel system, and the corresponding lipid channel system (with permission[27]). (B) Small angle x-ray scattering (SAXS) data for the cubic mesophase for phytantriol in the presence of aqueous 20 mM KCl.

As a particular feature, the $Pn\bar{3}m$ phase has two independent non-intersecting water channel systems. Due to this unique structural feature and the thermodynamic stability in excess water conditions,[17] the $Pn\bar{3}m$ cubic mesophase is promising for many applications. These range from use in pharmaceutical sciences for drug delivery vessels[18-20] and biosensors,[21-24] to materials templates for fuel cells,[25-27] solar cells,[28,29] and for photonic crystals.[30-33] When combined with a “capping agent”, phytantriol

[a] Rosemary Brown, Dr. James M. Stone, Dr. Kei Takashina, Department of Physics and Astronomy, University of Bath, Bath BA2 7AY, UK
[b] Dr. Elena Madrid, Dr. Remi Castaing, Prof. Karen J. Edler, Prof. Frank Marken Department of Chemistry, University of Bath, Bath BA2 7AY, UK (E-mail f.marken@bath.ac.uk)
[c] Dr. Adam M. Squires, Department of Chemistry, University of Reading, Whiteknights, Reading, RG6 6AD, UK

can be converted into stable “cubosome” or “hexosome” particles.[34,35] Key to mesophase properties and to applications is the ionic transport through the water channels. Therefore it is important to develop new approaches for the study of transport properties of the $Pn\bar{3}m$ mesophase material and for the study of phenomena associated with phase transformation.

Ion transport through the mesophase of phytantriol can be quantified as resistivity and can be affected by the ionic strength and by the specific interactions of ions with the hydrophilic head groups of the lipid. In order to study ion flow in the lipid mesophase materials, phytantriol-modified electrodes have been previously employed with a redox probe molecule.[23] However, the resulting redox processes coupled to transport in the mesophase are complicated. In fact, the redox process is likely to directly affect the ionic conductivity in mesophase channels. Studies based on free-standing lyotopic lipid phases have been reported by Speziale et al.[36] for monolinolein lyotropic phase and for the reconstitution of membrane proteins. Here, a similar approach is selected, but based on a microhole geometry and with four-electrode microhole voltammetry to apply a well-defined potential across a “free-standing” phytantriol film supported on a polymer substrate. Figure 2 shows a schematic drawing of the two-compartment electrochemical cell with a poly-ethylene-terephthalate (PET) film with microhole separating the two sides. This kind of measurement cell is employed commonly in liquid-liquid interface studies[37,38] or membrane characterisation[39] and employed here for the investigation of phytantriol mesophase films.

In this study, phytantriol is applied either to a single side (asymmetric) or to both sides (symmetric) of the PET film and equilibration in aqueous electrolyte then produces the mesophase as a film of typically 100 μm thickness. Recently, in a similar approach intrinsically microporous polymers (PIMs) have been investigated with microhole voltammetry based on a 6 μm thin poly-ethylene-terephthalate (PET) film with a laser-drilled approximately 20 μm diameter microhole.[40,41] By depositing the meso- or microporous samples onto the microhole, a well- defined potential can be applied across the sample (employing the four-electrode configuration, see Figure 2) and ion flow can be investigated with low bias or with high bias methods. Transport of ions towards the microhole (via spherical or convergent diffusion) can be assumed to be fast so that phenomena in (or in the vicinity of) the microhole are rate-limiting during the measurement.

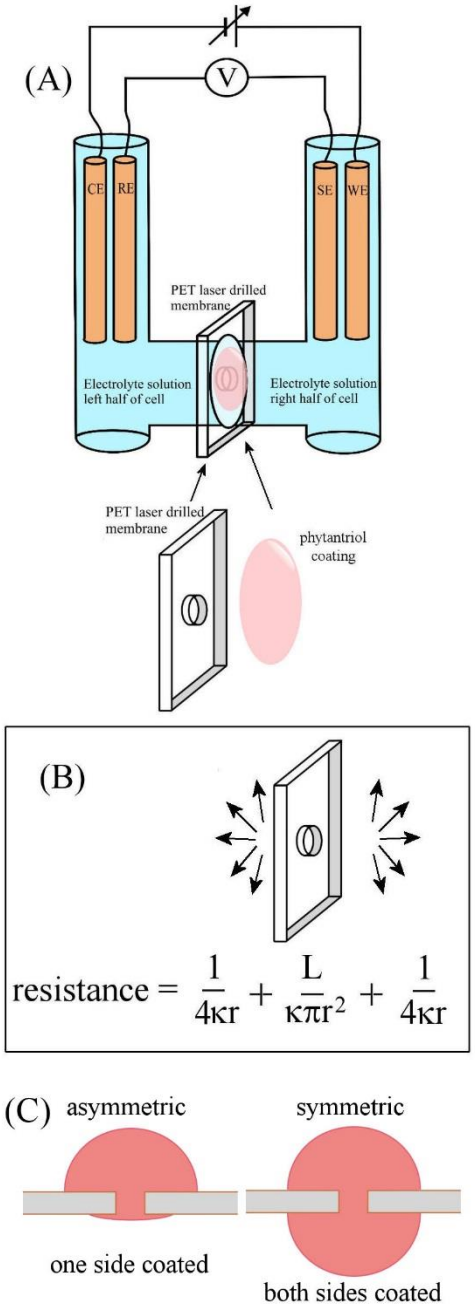

Figure 2. (A) Schematic drawing (not to scale) of a four-electrode electrochemical cell (CE = counter electrode, RE = reference electrode, SE = sense electrode, WE = working electrode) with poly-ethylene-terephthalate film (PET, laser-drilled) to support the phytantriol phase. Both asymmetrical (lipid on one side) and symmetric (lipid on both sides) experiments were performed. (B) Scheme to explain the three components in the resistance of the microhole with κ, the specific conductivity, L, the PET film thickness, and r, the microhole radius. (C) Schematic drawing of the “asymmetric“ and “symmetric“ deposits of phytantriol on PET.

This report describes a method that can be employed to observe ion transport and possible current rectification phenomena in the cubic mesophase of phytantriol. The ions measured in this study are potassium, K^+, and chloride, Cl^-, which are relatively small (covalent diameter for K^+ 0.266 nm for Cl^- 0.362 nm[42] compared

to the typical phytantriol channel diameter 2.2 nm[43]) and may be regarded as typical of an inert background electrolyte with approximately equal transference.[44] KCl is not expected to have any significant interactions with the uncharged lipid[27] (apart from water channel constriction and dehydration effects at very high concentration), and so any changes in ion transport from bulk solution are predominantly due to the cubic mesophase channel structure and behaviour. In the experiment, pure phytantriol was applied to the pore either in symmetrical fashion (right hand side and left hand side) or as asymmetric deposit applied from a single side (only on the right hand side, consistent with the side where the working electrode is placed, see Figure 2). The cubic phase forms *in situ* (within 24 h) upon addition of aqueous KCl solution to the measurement cell. Figure 1B confirms the formation of the cubic phase (typical diffraction peaks are indicated) for phytantriol in contact to excess aqueous 0.01 M KCl solution. After 24 h equilibration, applied potential (employing voltammetry or impedance methods) causes ions to flow through the cubic phase from one side of the cell to the other. This report contrasts experiments with low and with high applied bias and as a function of temperature. Novel features in ion conductivity are observed such as room temperature switching between two different microhole conductivity states and reversible switching during the thermally induced Q^{224} to H_{II} phase transition.

Table 1. Resistance and specific conductance values (T = 20 ± 2 °C; errors estimated) measured for Q^{224} mesophase of phytantriol applied symmetrically to a PET substrate with microhole (see text).

	Voltammetry: Symmetrical Deposit of Q^{224} Phase		Impedance: Symmetrical Deposit of Q^{224} Phase	
[KCl] / M	R / Ω [a]	κ / $\Omega^{-1}m^{-1}$ [b]	R / Ω [a]	κ / $\Omega^{-1}m^{-1}$ [b]
0.5	397×10^3 (± 1%)	186×10^{-3}	401×10^3 (± 1%)	184×10^{-3}
0.2	822×10^3 (±10 %)	89.7×10^{-3}	902×10^3 (± 1%)	81.8×10^{-3}
0.05	5.26×10^6 (± 1%)	14×10^{-3}	5.38×10^6 (± 1%)	13.7×10^{-3}
0.02	1.41×10^7 (± 2%)	5.23×10^{-3}	1.38×10^7 (± 1%)	5.34×10^{-3}
0.005	5.05×10^7 (± 3%)	1.46×10^{-3}	5.07×10^7 (± 1%)	1.45×10^{-3}
0.002	7.43×10^7 (± 2%)	0.99×10^{-3}	7.29×10^7 (± 2%)	1.01×10^{-3}

[a] measured resistance. [b] specific conductivity obtained with the equation given in Figure 2B.

Results and Discussion

Low Bias Electrochemical Characterization. In order to obtain information about ionic conductivity of the cubic phase, initially experiments are discussed that were performed at low applied bias potentials (due to higher applied bias potentials causing disruption of the asymmetric phytantriol deposit). When voltammetric experiments were performed within a +/-0.8 V window, stable Ohmic current responses (see Figure 3a) were obtained. Initially, only the empty microhole was employed in aqueous KCl electrolytes solutions as a calibration approach. Data from these measurements are plotted in Figure 3b (black squares). Good linearity with KCl concentration is observed. An approximate expression for the corresponding resistivity in the microhole[45] can be based on three contributions from (i) the left hemisphere, (ii) the cylindrical core, and (iii) the right hemisphere (see Figure 2B). Fitting the experimental resistance results to literature data for aqueous KCl conductivity at 20 °C[46] allowed the microhole radius r = 9.5 μm (see equation in Figure 2B) to be calibrated (assuming a PET film thickness of L = 6 μm and ignoring other geometric imperfections produced in the laser-drilling process). This value is in excellent agreement with the nominal diameter. Once the microhole is calibrated, the equation allows conversion of any measured resistance for a bulk ion conductor deposited symmetrically around the microhole (here for phytantriol mesophase) into value of specific conductance κ (in $\Omega^{-1}m^{-1}$; see Table 1; *vide infra*).

Low bias measurements were employed to characterise and compare four cases: (i) the empty microhole in aqueous KCl, and (ii) the asymmetrically coated mcirohole, and (iii) again the asymmetrically coated microhole but exposed to high bias, and (iv) the symmetrically phytantriol-coated microhole with phytantriol Q^{224} phase equilibrated immersed in aqueous KCl. Cyclic voltammograms were performed from -0.8 V to +0.8 V in KCl solutions of different concentration. Figure 3a shows typical cyclic voltammograms that exhibited linear resistive (Ohmic) behaviour for both symmetric and asymmetric phytantriol deposits. The gradient at zero current was used to obtain a resistance value. This linear behaviour was observed for each concentration (see Figure 3b) consistent with simple partitioning of electrolyte into the mesophase material. Conductivity data for the symmetric phytantriol case are summarised in Table 1. The presence of phytantriol mesophase clearly increases the resistance (or decreases the specific conductivity) by a factor of typically 30-40, which is a factor here attributed to the presence of the water channel system in the mesophase. Due to the microhole geometry the measurement is localized and insensitive to the phytantriol layer thickness.

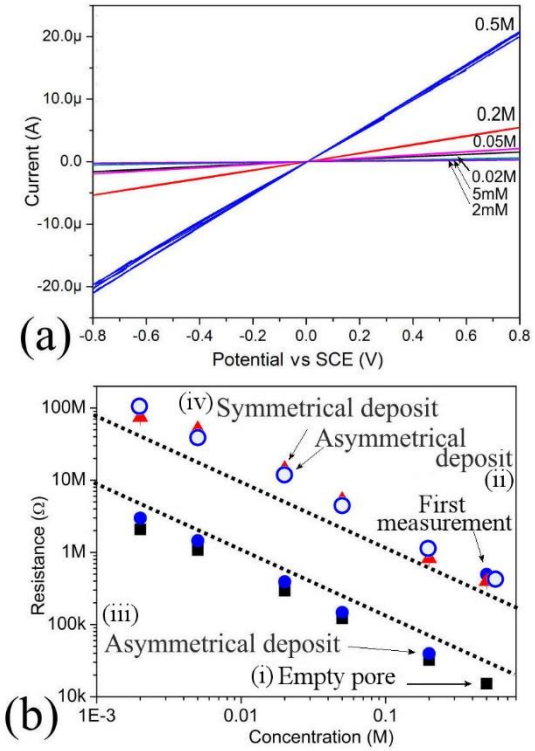

Figure 3. (a) Low bias cyclic voltammograms (3 cycles; scan rate 0.02 Vs^{-1}) for an asymmetric phytantriol deposit onto a 20 μm diameter microhole in PET immersed in 0.002, 0.005, 0.02, 0.05, 0.2, 0.5 M aqueous KCl. (b) Resistance data calculated from the slope of cyclic voltammetry data for (i) an empty microhole, (ii) an asymmetric phytantriol deposit, (iii) an asymmetric phytantriol deposit but employing large bias in between measurements, and (iv) a symmetric deposit with phytantriol on both sides of the microhole. An important "history effect" is noted where the *first measurement* for the asymmetric deposit appears in the high resistance domain with all following measurements in the low resistance domain. This effect is caused by high bias experiments "switching" the asymmetric deposit of phytantriol to a lower resistance (*vide infra*).

For asymmetric deposits (see Figure 3bii) low bias data suggests a resistance very similar to that for the filled microhole. However for asymmetric deposits and when employing high bias conditions in between measurements, the interpretation of data is much less straight forward. In the first measurement (see Figure 3biii) the resistance of the empty pore is low compared to the resistance for both symmetrically or asymmetrically phytantriol-filled pores. This suggests that also for the asymmetrically deposited phytantriol the microhole is essentially filled up with mesophase. However, in the following measurements the resistance for the empty microhole and for the asymmetric deposit appear very similar due to a "history" effect linked to loss of phytantriol from the microhole. This "switch" in behaviour is caused by high bias measurements (performed sequentially with low bias experiments) essentially emptying the microhole in between measurements. When high bias experiments were performed the resistance for asymmetric deposit considerably lowered affecting all the following data points. This effect continued for measurements performed with impedance spectroscopy (see Figure 4). However, this "history" effect is not observed for symmetrically deposited phytantriol films (see Figure 3biv) and for the asymmetric deposit when avoiding high bias experiments (see Figure 3bii).

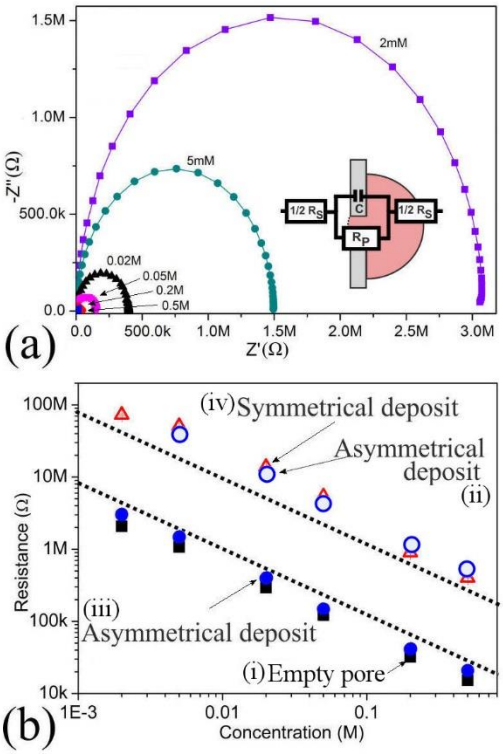

Figure 4. Low bias characterization obtained with impedance spectroscopy (amplitude 200 mV, frequency range 1 Hz to 40 kHz). (a) Nyquist plots for varying KCl concentration shown for an asymmetric mesophase deposit. (b) Summary of R_p data obtained with impedance spectroscopy for (i) an empty microhole, (ii) an asymmetric phytantriol deposit, (iii) an asymmetric phytantriol deposit but employing high bias in between measurements, and (iv) a symmetric deposit with phytantriol on both sides of the microhole. Note that the resistance for the asymmetric deposit is lowered due to a "history effect" when employing high bias in between measurements (see text).

Impedance measurements were performed in four-electrode configuration similar to measurements reported previously for liquid | liquid interfaces.[47] Impedance measurements were performed with 200 mV amplitude at 0.0 V bias (1 Hz to 40 kHz) and resulted in classic RC semicircle Nyquist plots for all experiments. Figure 4a shows typical Nyquist plots for the asymmetrical deposit, and similar behaviour was found for the symmetrical regime (see Figure 4b). The inset shows the model used to fit the data, and how this relates to the experimental system. The high frequency intercept (at low Z') is associated with the solution resistance, R_S. The diameter of the semicircle is determined by the PET interfacial capacitance, with typically C = 0.6 nF (consistent with literature reports[40]) and the resistance of the cubic phase inside the pore, R_P (ignoring any further

resistance contributions from the interface of cubic phase to aqueous phase). Figure 4b shows how R_P changes with concentration for the lipid deposits. Resistance data obtained from impedance and from cyclic voltammetry measurements are in very good agreement and summarized in Table 1 for symmetric deposits.

The observation that the ionic conductivity for KCl in phytantriol is lower by a factor of 30-40 compared to that of pure aqueous electrolyte can be compared to some previous literature reports based on other types of experimental methods. However, reports are scarce and results sometimes contradictory. Anderson and Wennerström[48] found that in general, diffusion rates inside the cubic phase are typically 60-70 % lower compared to the bulk solution diffusion rate. The diffusion rate for the ferrocyanide/ ferricyanide redox system has been reported to be retarded by a factor either 2-4,[49,50] or a factor of 200,[51] depending on the measurement technique chronocoulometry or impedance spectroscopy. When assuming the lipid phase as an impenetrable obstacle in the diffusion path of cations and anions, it is possible to express the effective diffusivity D_{eff} (eq. 1)[52].

$$D_{eff} = \frac{\varepsilon}{\tau} D \qquad (1)$$

In this expression the effective diffusion coefficient is given by the real diffusion coefficient multiplied by ε, the valid fraction (here the water fraction for Q^{224} approximately 0.26 – 0.28 and for H_{II} approximately 0.20 – 0.26 [53]), and τ, the tortuosity. The specific conductivity κ_{eff} in this case can also be expressed (eq. 2).

$$\kappa_{eff} = c\, D_{eff} \frac{F^2}{RT} = c\, D \frac{\varepsilon}{\tau} \frac{F^2}{RT} \qquad (2)$$

Experimental values of $\frac{\tau}{\varepsilon}$ of 30-40 reported here therefore suggest a tortuosity of approximately τ = 10. There is another strong increase in tortuosity when switching from cubic Q^{224} to hexagonal H_{II} phase (*vide infra*).

High Bias Electrochemical Characterisation. In order to explore physico-chemical phenomena, in particular the asymmetric mesophase deposit at higher potential bias, an extended ±4 V potential range was studied by cyclic voltammetry (see Figure 5). Data for 10 mM KCl electrolyte are shown, but generally for all concentrations more complex (non-Ohmic) asymmetric current traces are observed. In contrast to the Ohmic behaviour observed for experiments with smaller bias, here non-linearity is clearly observed particularly in the negative potential range. When scanning the potential into the positive potential range only small deviation from Ohmic behaviour are seen (Figure 5c), but when scanning the potential into the negative range, the current increases dramatically and it loops to give even higher currents during the return of the potential to zero. Additional noise on the current signal suggests phase transformation/disruption effects. When this experiment is performed *in situ* in an optical microscope to monitor the microhole during the voltammetry experiment, there is clear evidence for the initially clear pore (under positive potential conditions) going dark with "spots" of material appearing around the microhole under negative potential conditions. It can be concluded that some phytantriol is expelled from the microhole (thereby lowering the resistance) and probably propelled out into the aqueous solution phase (see Figure 5).

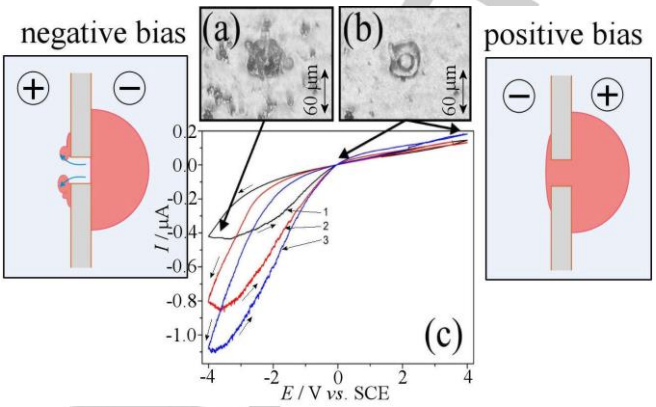

Figure 5. Optical micrographs of the micropore with asymmetric deposit in 10 mM KCl (a) during cyclic voltammogram at -4 V and (b) before conducting the cyclic voltammetry and in the positive potential region. (c) Cyclic voltammograms (scan rate 10 mVs^{-1}) for three consecutive potential cycles with increasing currents.

These observations can be considered as a bi-stable switching process. When high bias voltammetry scans are performed, a change in the "resistance state" of the asymmetrical deposit is observed at negative potentials. A "switch" appears to occur from high resistance to low resistance. The relaxation back to the original state is relatively slow (see Figure 6) if un-aided by applied positive potential. This suggests that the asymmetrical mesophase deposit was initially in the high resistance state (similar to the symmetrically coated micropore), but can be "switched" into the lower resistance state by the application of high negative bias (and emptying the microhole). The state is switched back by high positive bias. It is interesting to explore the relaxation processes associated with these two resistance states (Figure 6).

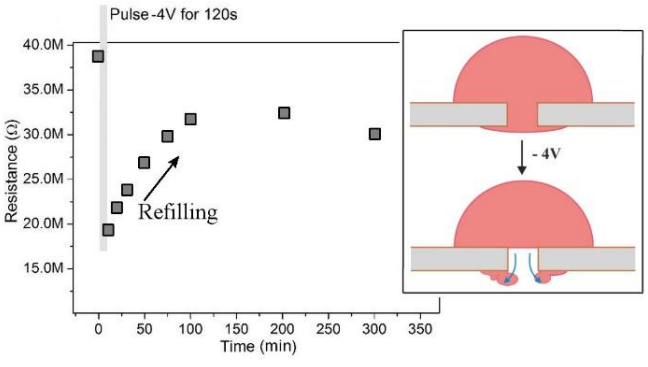

Figure 6. Plot of the resistance R_p for an asymmetric phytantriol mesophase deposit 10 mM KCl as a function of time (monitored by impedance spectroscopy at 0.0 V). After a single voltage pulse at -4 V for 120 s the slow relaxation back to high resistance is monitored. Also shown is a schematic drawing indicate the process of micropore emptying and re-filling.

Resistance data were measured systematically as a function of time after a voltage pulse at -4 V for 120 seconds has been applied for the asymmetrical phytantriol mesophase deposit. The first resistance value is the resistance of the pore before the pulse (Figure 6). The negative pulse lowered the pore resistance from a higher resistive state (40 MOhm; note that this consistent with a partially filled microhole; see Figure 3) to a lower state (20 MOhm). Following this, impedance measurements showed that the pore resistance relaxed back within a time period of 90 minutes. It is possible to explain this behaviour with the slow re-filling of the microhole with phytantriol Q^{224} phase (back to a lower energy equilibrium). A secondary relaxation process occurs on a much longer timescale (5 h to 24 h) which is seen as an additional lowering of the resistance in the background (possibly due to more loss of phytantriol).

Upon application of a high positive bias pulse, the resistance of the microhole can be "switched back". To explore this effect further, chronoamperometry (CA) was used to apply a constant potential at +4 V or -4 V. The potential was applied for 120 s every ten minutes, and impedance spectroscopy was used to 'read out' the resistive state of the pore. Figure 7 shows that CA potential pulses every ten minutes and the current response during the applied potential. The pulses correspond to the resistance R_p values plotted in Figure 7b where the black squares show the resistance post +4 V and the red squares those post -4 V. The applied potential can switch the pore from an open/empty state into a closed/filled state, forming a primitive volatile memory device.

Electrochemical Monitoring of Phase Changes. The switch in resistivity with applied bias voltage suggests structural changes, which have been linked with an "opening" and "closing" of the microhole. A further potential switching mechanism could be based on a localized phase transition (switching between two different mesophase geometries) and therefore additional exploration of the effect of temperature on the microhole resistance is necessary. Temperature effects on lipid mesophase structure are well studied[51] and phase switching for example in cubosomes,[54] hexosomes,[55] or in bulk with IR radiation have been reported.[56] There is no previous report on resistivity monitoring by electrochemical methods of phytantriol phase transitions.

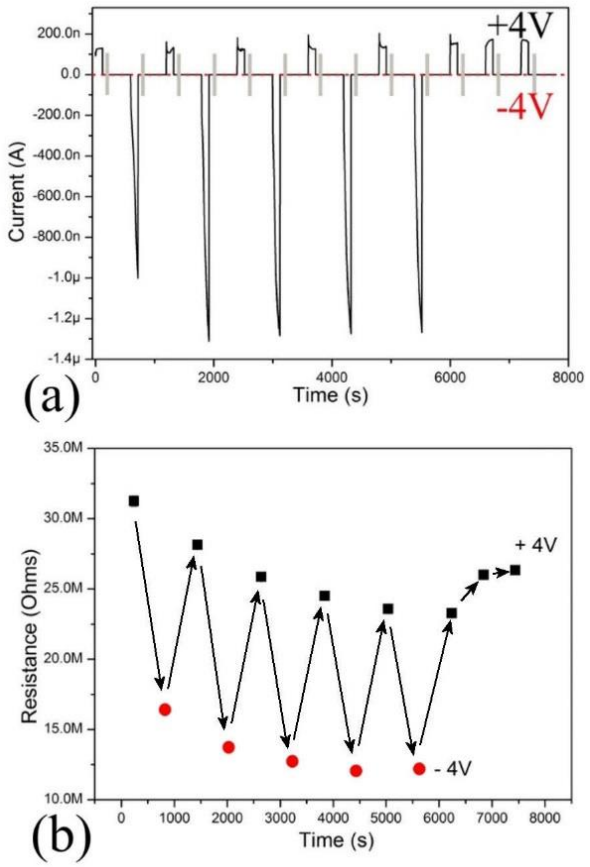

Figure 7. (a) Chronoamperometry data obtained for an asymmetrically deposited phytantriol mesophase in aqueous 10 mM KCl with 120 s pulses of +4 V and -4 V switching the pore resistance between a higher and lower resistive state. Grey bars indicate the read-out period. (b) Plot of the R_p read out data versus time.

Experiments were performed by slowly increasing the solution temperature and monitoring the impedance for a symmetric phytantriol mesophase deposit. Figure 8 shows the switch from less resistive Q^{224} cubic phase to the more resistive H_{II} hexagonal phase for two repeat measurements. The transition temperature of approximately 42 °C is reasonably consistent with some literature reports for phytantriol phase switching. It has been pointed out by Dong and coworkers that small levels of impurities in commercial phytantriol can cause a significant lowering of this phase transition temperature (here a 96 % pure phytantriol is employed), which is likely to explain discrepancies to some other reports.[57] For pure phytantriol the Q^{224} to H_{II} transition can occur at temperatures up to 15 °C higher (see phase diagram in Figure 8C). The significant increase in resistance when switching from Q^{224} cubic phase to the more resistive H_{II} hexagonal phase is in agreement with the essentially uni-directional cylindrical water channels in the hexagonal phase causing a major obstruction and change in tortuosity to impede ion transport.

The transition, when monitored by resistivity measurements, appears to occur associated with relaxation phenomena with distinct time constants. Initially (see first temperature scan in Figure 8A) when heating up the sample, the expected lowering of the resistivity mainly due to the increase in ion mobility is observed. At approximately 42 °C a phase transformation occurs very rapidly. Transformations of this type can occur via disruptive processes[58] linked to the break-down of one channel geometry and the gradual re-ordering of the product channel structure associated with water exchange and domain growth. A rapid rise of resistivity beyond 100 MOhm is clearly linked to the formation of the hexagonal phase. However, the process is complex and upon lowering the temperature and repeating the experiment slightly different behaviour is seen (Figure 8A). The complete phase conversion as well as the re-generation of the original Q^{224} mesophase equilibrium structure upon cooling may be slow and incomplete on the time scale of the experiment. Data in Figure 8B confirms that repeated switching of the phytantriol phase is possible in a 20 minute time scale.

The investigation of the effect of temperature increase and decrease on the specific conductivity of phytantriol mesophase offers a new insight into the phase transition process. Co-existence of phases[59] has been suggested and clearly the Q^{224} to H_{II} to Q^{224} transitions are not fast/clean and possibly associated with intermediates, water expulsion, and/or domain growth. However, due to the significant change in tortuosity when going from Q^{224} to H_{II}, there is a significant increase in resistance associated with the phase transition as a characteristic signature. Further work will be required for example better investigating the R_p – T dependence as a function of time and with varying salt concentrations or employing *in situ* diffractometry tools. These results could be important also from the viewpoint of drug release and future sensing applications.

In order to verify the phase transformation additional Differential Scanning Calorimetry (DSC) data were obtained. The Q^{224} cubic phase material was equilibrated in aqueous 10 mM KCl and then loaded into a closed hastelloy pan for thermal cycling. Figure 9A shows typical heating – cooling data sets obtained at four different temperature scan rates. The onset for the Q^{224} to H_{II} transition under these conditions is at 44 °C, which is in reasonable agreement with the electrochemical data. The transition appears to occur over a 5 °C range, which may be linked to formation of a separate water phase (which contrasts to conditions in the electrochemical experiment, which was performed in excess water).

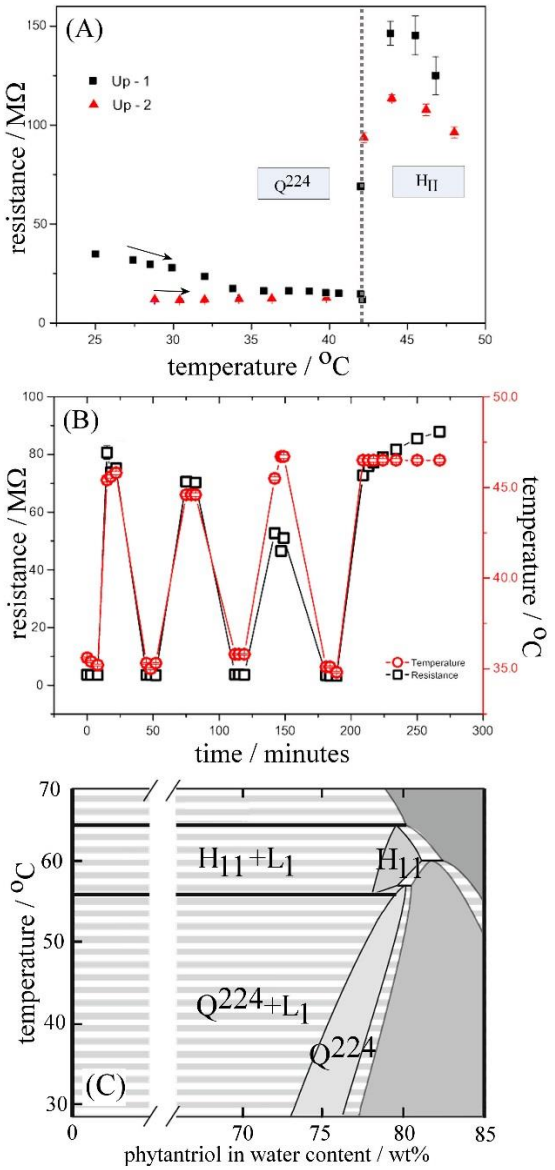

Figure 8. (A) Plot of resistance R_P data (from impedance experiments in 10 mM KCl) as a function of solution temperature for two consecutive temperature scans. When increasing the temperature the first time (black squares) and the second time (red triangles) the Q^{224} to H_{11} transition is observed at 42 °C. (B) Temperature switching between 35 °C and 45 °C allows continuous phase switching of phytantriol immobilized symmetrically onto the PET film. (C) Phase diagram for phytantriol-water adapted from Latypova et al.[60] with L_1 denoting an isotropic aqueous phase.

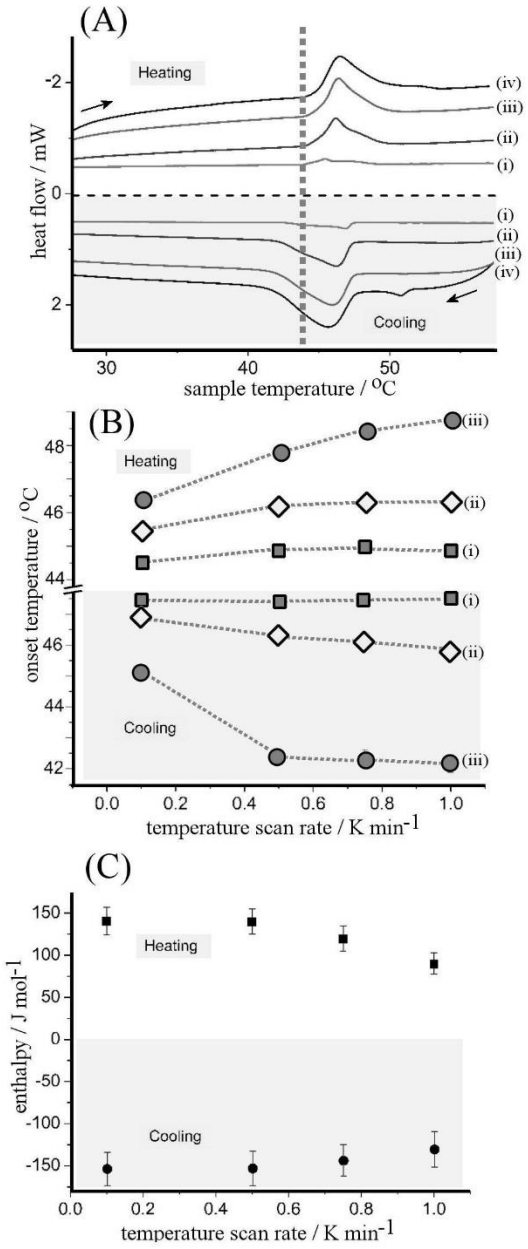

Figure 9. (A) Differential scanning calorimetry data for heat flow (for scan rates of (i) 0.1, (ii) 0.5, (iii) 0.75, and (iv) 1.0 K min^{-1}) for a 10 mM KCl hydrated phytantriol sample. Dashed line shows the onset of cubic to hexagonal phase transition. (B) Onset, peak, and end point for heating and cooling transitions as a function of scan rate. (C) Enthalpy data for cubic to hexagonal phase transition.

The onset, peak, and offset temperatures for the phase transition can be found (Figure 9B) as well as the enthalpy (estimated here as 0.5 mJ mg^{-1} or 150 J mol^{-1} based on phytantriol) from integrating the heat capacity curve (Figure 9C). Literature microcalorimetry data for phytantriol mesophase systems were reported by Doo-Hoon[61] on cubosomes. However, transition data were not unequivocally assigned as cubic to hexagonal. Reese and coworkers[62] found that the same type of transition in monoolein cubic phase was associated with an enthalpy of approximately 1.0 mJ mg^{-1}, very similar to the value of 0.5 mJ mg^{-1} reported here. Likewise, Cezelik and coworkers[63] suggested that the enthalpy change for the phase transition in monoolein in excess water is typical for a transition producing more fluid-like hydrocarbon chains.

Conclusions

A new approach to the study of ion flow and conductivity in mesophase materials has been introduced based on a microhole in a PET film assembled between two electrochemical half-cells in 4-electrode configuration. Both voltammetry and impedance experiments have been performed and the cases of (i) empty microhole, (ii) asymmetrically phytantriol-coated microhole, and (iii) symmetrically phytantriol-coated microhole are compared. Low potential bias data suggest a 30-40 times higher resistance in phytantriol Q^{224} mesophase material when compared to pure aqueous electrolyte. This can be explained based on tortuosity in the bicontinuous phase limiting ion transport. When investigating the reversible temperature induced phase transformation from Q^{224} to H_{II} phase and back, a significant further increase in resistivity for H_{II} is noted due to the even more tortuous water channel structure in the hexagonal phase. Behaviour appears to be associated with a disruptive phase transition with electrolyte exchange and mesophase domain formation, which will need further study possibly also as a function of the type of electrolyte. When studying high potential bias perturbation, microhole resistivity switching was observed and apparently reversible switching caused a “memory” effect with read-out of the “open” or “closed” state by impedance. Further work will be required to develop a better understanding of these processes and experiments *in situ* coupling x-ray diffraction techniques to electrochemistry will be desirable. Applications could be developed in sensing (exploiting the thermal phase transition as a sensitive probe) or for drug release. Most importantly, the symmetrically film-modified microhole appears to provide a convenient new probe for the study of conductivity and mesophase reactivity for a much broader range of materials and processes.

Experimental Section

Chemical Reagents. KCl (Sigma Aldrich) solutions of differing concentrations (500 mM, 200 mM, 50 mM, 20 mM, 5 mM, 2 mM) were prepared using ultra-pure filtered water of resistivity 18.2 MOhm cm. Phytantriol (a gift from Adina Ltd.) was used in commercial grade (96 %) without further purification, which has implications on the behaviour during phase transformation (*vide infra*).

Instrumentation. An Autolab potentiostat system (PGSTAT12, EcoChemie, The Netherlands) using the GPES control software was

employed with Pt wires as counter/working electrodes, and two KCl-saturated calomel reference electrodes (SCE, Radiometer, Copenhagen) as sense and reference in a metal Faraday cage. A Solartron 1260A/1286 impedance analyser system was used (amplitude 200 mV, frequency range 1 Hz to 40 kHz) with Z-View and Z-Plot software for impedance measurements and for data analysis.

A custom made U-shaped glass cell (Figure 2) was used that split in two and could be clamped together with a flange holding the membrane. For temperature control a U-shaped glass cell with thermostated jacket was employed with a Haake recirculating heating unit. This allowed for a 6 μm thick poly-ethylene-terephthalate (PET) membrane with a laser-drilled approximately 20 μm diameter hole (supplied by Laser Micromachining Limited, St. Asaph, Denbighshire LL17 0JG, UK) to be clamped between the two flange connectors of the cell. The microhole was used empty for reference/calibration measurements without the lipid. To apply the lipid to the pore, a pipette tip was dipped into the phytantriol bottle and a small amount (~6 mg) was then applied to the area of the PET membrane, where the microhole was located. The lipid layer was placed on the right hand side of the cell (together with the sensor and working electrode). Voltammetry and impedance experiments were performed for both the microhole empty and covered with lipid mesophase. For steady state voltammetry a scan rate of 0.02 Vs^{-1} was applied. For impedance measurements, the root mean squared voltage (V_{RMS}) or amplitude was 200 mV with a DC voltage of 0.0 V. Experiments were performed at 20 ± 2 °C. Small angle x-ray scattering (SAXS) measurements were performed with a paste cell for a 20 hour SAXS measurement in an Anton Paar PW3830 SAXSees system with a wavelength of 0.1542 nm verifying the formation of the cubic mesophase. Differential scanning calorimetry (DSC) was performed using phytantriol immersed in excess 10 mM KCl. About 300 mg of the cubic phase was placed into Hastelloy cells in a Seteram heat flow Micro-DSC. Reference Hastelloy cells contained approximately 100 μL of aqueous KCl solution. The temperature was swept from 25 °C to 65 °C at four different sweep rates with 0.1, 0.5, 0.75 or 1.0 °C min^{-1}. For *in situ* optical microscopy a custom-made Teflon cell consisting of two Teflon blocks with a circular cavity in the centre was designed for use with a GXML 3230 confocal microscope with a GXCAM USB camera. The PET membrane was sandwiched between the two Teflon blocks with two glass slides on the outer edges to form a transparent cylindrical vessel. The electrolyte solution was injected and two platinum wires acted as counter and working electrodes along with two silver wires as the quasi-sensor and quasi-reference electrodes.

Acknowledgements

We acknowledge financial support from the EPSRC (EP/K004956/1).

Keywords: Impedance • Voltammetry • Mesophase • Conductivity • Memory

[1] A. Iglic, *Advances in Biomembranes and Lipid Self-Assembly*. Academic Press, New York, **2016**.

[2] R. H. Dong, W. M. Liu, J. C. Hao, Soft vesicles in the synthesis of hard materials. *Acc. Chem. Res.* **2012**, *45*, 504-513.

[3] B. R. Wiesenauer, D. L. Gin, Nanoporous polymer materials based on self-organized, bicontinuous cubic lyotropic liquid crystal assemblies and their applications. *Polym. J.* **2012,** *44*, 461-468.

[4] C. E. Conn, C. J. Drummond, Nanostructured bicontinuous cubic lipid self-assembly materials as matrices for protein encapsulation. *Soft Matter* **2013**, *9*, 3449-3464.

[5] M. Lapteva, T. N. Kalia, Microstructured bicontinuous phase formulations: their characterization and application in dermal and transdermal drug delivery. *Expert Opinion Drug Delivery* **2013**, *10*, 1043-1059.

[6] J. C. Shah, Y. Sadhale, D. M. Chilukuri, Cubic phase gels as drug delivery systems. *Adv. Drug Delivery Rev.* **2001**, *47*, 229-250.

[7] K. Larsson, Cubic lipid-water phases – structures and biomembrane aspects. *J. Phys. Chem.*, **1989**, *93*, 7304–7314

[8] E. Nazaruk, R. Bilewicz, G. Lindblom, B. Lindholm-Sethson, Cubic phases in biosensing systems. *Anal. Bioanal. Chem*. **2008**, *391*, 1569-1578.

[9] L. M. Antognini, S. Assenza, C. Speziale, R. Mezzenga, Quantifying the transport properties of lipid mesophases by theoretical modelling of diffusion experiments. *J. Chem. Phys.* **2016**, *145*, 084903.

[10] S. Aleandri, C. Speziale, R. Mezzenga, E. M. Landau, Design of light-triggered lyotropic liquid crystal mesophases and their application as molecular switches in "on demand" release. *Langmuir* **2015**, *31*, 6981-6987.

[11] R. Negrini, W. K. Fong, B. J. Boyd, R. Mezzenga, pH-responsive lyotropic liquid crystals and their potential therapeutic role in cancer treatment. *Chem. Commun*. **2015**, *51*, 6671-6674.

[12] R. Negrini, R. Mezzenga, pH-responsive lyotropic liquid crystals for controlled drug delivery. *Langmuir* **2011**, *27*, 5296-5303.

[13] J. J. Vallooran, R. Negrini, R. Mezzenga, Controlling anisotropic drug diffusion in lipid-Fe3O4 nanoparticle hybrid mesophases by magnetic alignment. *Langmuir* **2013**, *29*, 999-1004.

[14] R. Negrini, R. Mezzenga, Diffusion, molecular separation, and drug delivery from lipid mesophases with tunable water channels. *Langmuir* **2012**, *28*, 16455-16462.

[15] W. K. Fong, R. Negrini, J. J. Vallooran, R. Mezzenga, B. J. Boyd, Responsive self-assembled nanostructured lipid systems for drug delivery and diagnostics. *J. Coll. Interface Sci.* **2016**, *484*, 320-339.

[16] J. Barauskas, T. Landh, Phase behavior of the phytantriol/water system. *Langmuir*, **2003**, *19*, 9562–9565.

[17] U. S. Schwarz, G. Gompper, Bending frustration of lipid-water mesophases based on cubic minimal surfaces. *Langmuir*, **2001**, *17*, 2084–2096.

[18] J. Clogston, M. Caffrey, Controlling release from the lipidic cubic phase: Amino acids, peptides, proteins and nucleic acids. *J. Control. Release*, **2005**, *107*, 97–111.

[19] R. Negrini, R. Mezzenga, Diffusion, molecular separation, and drug delivery from lipid mesophases with tunable water channels. *Langmuir*, **2012**, *28*, 16455–16462.

[20] C. J. Drummond, C. Fong, Surfactant self-assembly objects as novel drug delivery vehicles. *Curr. Opin. Colloid Interface Sci.*, **1999**, *4*, 449–456.

[21] E. Nazaruk, R. Bilewicz, G. Lindblom, B. Lindholm-Sethson, Cubic phases in biosensing systems. *Anal. Bioanal. Chem.*, **2008**, *391*, 1569–1578.

[22] P. Rowiński, A. Korytkowska, R. Bilewicz, Diffusion of hydrophilic probes in bicontinuous lipidic cubic phase. *Chem. Phys. Lipids*, **2003**, *124*, 147–156.

[23] R. Bilewicz, P. Rowiński, E. Rogalska, Modified electrodes based on lipidic cubic phases. *Bioelectrochemistry*, **2005**, *66*, 3–8.

[24] J. Kostela, M. Elmgren, Redox activity and diffusion of hydrophilic, hydrophobic, and amphiphilic redox active molecules in a bicontinuous cubic phase. *J. Phys. Chem. B*, **2005**, *109*, 5073–5078.

[25] S. C. Price, X. Ren, A. C. Jackson, Y. Ye, Y. A. Elabd, F. L. Beyer, Bicontinuous alkaline fuel cell membranes from strongly self-segregating block copolymers. *Macromolecules*, **2013**, *46*, 7332–7340.

[26] J. Lee, M. C. Orilall, S. C. Warren, M. Kamperman, F. J. DiSalvo, U. Wiesner, Direct access to thermally stable and highly crystalline

mesoporous transition-metal oxides with uniform pores. *Nat. Mater.*, **2008**, *7*, 222–228.

[27] S. Akbar, J. M. Elliott, M. Rittman, A. Squires, Facile production of ordered 3D platinum nanowire networks with "single diamond" bicontinuous cubic morphology. *Adv. Mat*, **2013**, *25*, 1160–1164.

[28] E. J. W. Crossland, M. Kamperman, M. Nedelcu, C. Ducati, U. Wiesner, D. M. Smilgies, G. E. S. Toombes, M. A. Hillmyer, S. Ludwigs, U. Steiner, H. J. Snaith, A bicontinuous double gyroid hybrid solar cell. *Nano Lett.*, **2009**, *9*, 2807–2812.

[29] H. Wang, C. C. Oey, A. B. Djurišić, M. H. Xie, Y. H. Leung, K. K. Y. Man, W. K. Chan, A. Pandey, J. M. Nunzi, P. C. Chui, Titania bicontinuous network structures for solar cell applications *Appl. Phys. Lett.*, **2005**, *87*, 023507.

[30] D. R. Dunphy, F. L. Garcia, B. Kaehr, C. Y. Khripin, A. D. Collord, H. K. Baca, M. P. Tate, H. W. Hillhouse, J. W. Strzalka, Z. Jiang, J. Wang, C. J. Brinker, Tricontinuous cubic nanostructure and pore size patterning in mesostructured silica films templated with glycerol monooleate. *Chem. Mater.*, **2011**, *23*, 2107–2112.

[31] W. Yue, W. Zhou, Porous crystals of cubic metal oxides templated by cage-containing mesoporous silica *J. Mater. Chem.*, **2007**, *17*, 4947–4952.

[32] J. A. Dolan, B. D. Wilts, S. Vignolini, J. J. Baumberg, U. Steiner, T. D. Wilkinson, Optical properties of gyroid structured materials: from photonic crystals to metamaterials. *Adv. Opt. Mater.*, **2014**, *3*, 12-32.

[33] L. Lu, L. Fu, J. D. Joannopolous, M. Solijacic, Weyl points and line nodes in gyroid photonic crystals. *Nat. Photonics*, **2013**, *7*, 294–299.

[34] T. E. Hartnett, K. Ladewig, A. J. O'Connor, P. G. Hartley, K. M. McLean, Size and phase control of cubic lyotropic liquid crystal nanoparticles. *J. Phys. Chem. B*, **2014**, *118*, 7430-7439.

[35] A. W. Dong, C. Fong, L. J. Waddington, A. J. Hill, B. Boyd, C. J. Drummond, Application of positron annihilation lifetime spectroscopy (PALS) to study the nanostructure in amphiphile self-assembly materials: phytantriol cubosomes and hexosomes. *Phys. Chem. Chem. Phys.* **2015**, *17*, 1705-1715.

[36] C. Speziale, L. S. Manni, C. Manatschal, E. M. Landau, R. Mezzenga, A macroscopic H^+ and Cl^- ions pump via reconstitution of EcClC membrane proteins in lipidic cubic mesophases. *PNAS* **2016**, *113*, 7491-7496.

[37] M. C. Osborne, Y. Shao, C. M. Pereira, H. H. Girault, Micro-hole interface for the amperometric determination of ionic species in aqueous-solution. *J. Electroanal. Chem.*, **1994**, *364,* 155-161.

[38] A. J. Olaya, M. A. Mendez, F. Cortes-Salazar, H. H. Girault, Voltammetric determination of extreme standard Gibbs ion transfer energy. *J. Electroanal. Chem.*, **2010**, *644*, 60-66.

[39] J. S. Rossier, R. Ferrigno, H. H. Girault, Electrophoresis with electrochemical detection in a polymer microdevice. *J. Electroanal. Chem.*, **2000**, *492*, 15-22.

[40] E. Madrid, Y. Rong, M. Carta, N. B. McKeown, R. Malpass-Evans, G. A. Attard, T.J. Clarke, S. H. Taylor, Y. T. Long, F. Marken, Metastable Ionic Diodes Derived from an Amine-Based Polymer of Intrinsic Microporosity *Angew. Chem. Int. Ed. Engl.*, **2014**, *53*, 10751–10754.

[41] E. Madrid, P. Cottis, Y. Rong, A. T. Rogers, J. M. Stone, R. Malpass-Evans, M. Carta, N. B. McKeown, F. Marken, Water desalination concept using an ionic rectifier based on a polymer of intrinsic microporosity (PIM). *J. Mater. Chem. A*, 2015, *3*, 15849–15853.

[42] Y. Marcus, *Ion properties*. Marcel Dekker, New York, **1997**, p. 46.

[43] E. Nazaruk, P. Miszta, S. Filipek, E. Gorecka, E. M. Landau, R. Bilewicz, Lyotropic cubic phases for drug delivery: diffusion and sustained release from the mesophase evaluated by electrochemical methods. *Langmuir*, **2015**, *31*, 12753-12761.

[44] K. B. Oldham, J. C. Myland, *Fundamentals of electrochemical science*. Academic Press, New York, **1994**, p. 12.

[45] J. E. Hall, Access Resistance of a Small Circular Pore. *J. Gen. Physiol.*, **1975**, *66*, 531-532.

[46] W. F. Koch, Y. C. Wu, P. A. Berezansky, Molality-based primary standards of electrolytic conductivity - (IUPAC technical report). *Pure Appl. Chem.*, **2001**, *73*, 1783-1793.

[47] A. Trojanek, V. Marecek, Z. Samec, Some aspects of impedance measurements at the interface between two immiscible electrolyte solutions in the four-electrode cell. *Electrochim. Acta*, **2015**, *179*, 3-8.

[48] D. M. Anderson, H. Wennerström, Self-diffusion in bicontinuous cubic phases, L3 phases, and microemulsions. *J. Phys. Chem.*, **1990**, *94*, 8683–8694.

[49] J. Kostela, M. Elmgren, Redox activity and diffusion of hydrophilic, hydrophobic, and amphiphilic redox active molecules in a bicontinuous cubic phase. *J. Phys. Chem. B*, **2005**, *109*, 5073–5078.

[50] P. Rowiński, A. Korytkowska, R. Bilewicz, Diffusion of hydrophilic probes in bicontinuous lipidic cubic phase. *Chem. Phys. Lipids*, **2003**, *124*, 147–156.

[51] E. Nazaruk, R. Bilewicz, G. Lindblom, B. Lindholm-Sethson, Cubic phases in biosensing systems. *Anal. Bioanal. Chem.*, **2008**, *391*, 1569–1578.

[52] E. L. Cussler, *Diffusion – Mass Transfer in Fluid Ssytems*. Cambridge Univesrity Press, Cambridge **2003**, p. 173.

[53] J. Barauskas, T. Landh, Phase Behavior of the Phytantriol/Water System. *Langmuir*, **2003**, *19*, 9562–9565.

[54] B. W. Muir, G. L. Zhen, P. Gunatillake, P. G. Hartley, Salt induced lamellar to bicontinuous cubic phase transitions in cationic nanoparticles. *J. Phys. Chem. B*, **2012**, *116*, 3551-3556.

[55] A. Tilley, Y. D. Dong, H. Amenitsch, M. Rappolt, B. J. Boyd, Transfer of lipid and phase reorganisation in self-assembled liquid crystal nanostructured particles based on phytantriol. *Phys. Chem. Chem. Phys.*, **2011**, *13*, 3026-3032.

[56] M. D. J. Quinn, J. N. Du, B. Boyd, A. Hawley, S. M. Notley, Lipid liquid-crystal phase change induced through near-infrared irradiation of entrained graphene particles. *Langmuir*, **2015**, *31*, 6605-6609.

[57] Y. D. Dong, A. W. Dong, I. Larson, M. Rappolt, H. Amenitsch, T. Hanley, B. J. Boyd, Impurities in commercial phytantriol significantly alter its lyotropic liquid-crystalline phase behaviour. *Langmuir*, **2008**, *24*, 6998-7003.

[58] A. M. Squires, S. Akbar, M. E. Tousley, Y. Rokhlenko, J. P. Singer, C. O. Osuji, Experimental evidence for proposed transformation pathway from the inverse hexagonal to inverse diamond cubic phase from oriented lipid samples. *Langmuir*, **2015**, *31*, 7707-7711.

[59] A. Angelova, M. Ollivon, A. Campitelli, C. Bourgaux, Lipid cubic phases as stable nanochannel network structures for protein biochip development: X-ray diffraction study. *Langmuir*, **2003**, *19*, 6928-6935.

[60] L. Latypova, W. Gozdz, P. Pieranski, Symmetry, topology and faceting in bicontinuous lyotropic crystals. *Eur. Phys. J. E* **2013**, *36*, 88.

[61] D. H. Kim, S. Lim, J. Shim, J. E. Song, J. S. Chang, K. S. Jin, E. C. Cho, A simple evaporation method for large-scale production of liquid crystalline lipid nanoparticles with various internal structures. *ACS Appl. Mater. Interf.*, **2015**, *7*, 20438-20446.

[62] C. W. Reese, Z. I. Strango, Z. R. Dell, S. Tristram-Nagle, P. E. Harper, Structural insights into the cubic-hexagonal phase transition kinetics of monoolein modulated by sucrose solutions. *Phys. Chem. Chem. Phys.*, **2015**, *17*, 9194-9204.

[63] C. Czeslik, R. Winter, G. Rapp, K. Bartels, Temperature-dependent and pressure-dependent phase-behaviour of monoacylglycerides, monoolein and monoeladin. *Biophys. J.* **1993**, *68*, 1423-1429.

Entry for the Table of Contents (Please choose one layout)

ARTICLE

Micropore ionic conductivity measurement and switching

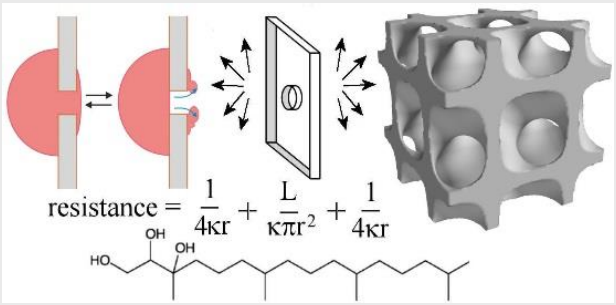

*Rosemary Brown, Elena Madrid, Remi Castaing, James M. Stone, Adam M. Squires, Karen J. Edler, Kei Takashina, Frank Marken**

Page No. – Page No.

Free-Standing Phytantriol Q^{224} Cubic Phase Films: Resistivity Monitoring and Switching